

Morphological evolution of lingulids (Brachiopoda): How did ecological opportunist adapt to harsh marine environments in the Early Triassic?

Huiting Wu ^{a,b}, Thomas L. Stubbs ^c, Anfeng Chen ^{d,e}, Xiujuan Wu ^a, Yang Zhang ^{d,*}

^a School of Geoscience and Surveying Engineering, China University of Mining and Technology, Beijing, China

^b State Key Laboratory of Palaeobiology and Stratigraphy, Nanjing Institute of Geology and Palaeontology, CAS, Nanjing, China

^c School of Life, Health and Chemical Sciences, The Open University, Walton Hall, Milton Keynes MK7 6AA, UK

^d School of Earth Sciences and Resources, China University of Geosciences (Beijing), Beijing, China

^e Natural History Museum of China, Beijing, China



ARTICLE INFO

Editor: S Shen

Keywords:

Early Triassic

Recovery

Lingulid brachiopod

Geometric morphometrics

Morphological disparity

Shell size

ABSTRACT

The Early Triassic fossil record is notoriously poor, and mostly composed of a few ecological opportunists and disaster taxa that are small marine invertebrates. Amongst them are inarticulate lingulid brachiopods that commonly appear in Early Triassic shallow-water sections worldwide, with high abundance. Lingulidae is a classic 'living fossil', normally considered as having unchanged 'linguliform' shape (elongate oval outline with subparallel or slightly curved lateral margins) since it first appeared in the Late Devonian. However, our morphometric analyses reveal subtle, but important, morphological adaptations of these opportunistic taxa during the Early Triassic, based on thousands of lingulid specimens from two shallow-water sections in South China. From the early Griesbachian to the early Smithian, lingulid shape changed to become slimmer, and by having narrower front ends and relatively wider posterior, and might more space to accommodate muscles posteriorly, which together, would make it easier to withdraw into, and protrude out from, their substrate shelters. These morphological changes could be related to increased predation intensity and sediment grain size in the studied sections, which would have negative impacts on the burrowing capability of lingulids. In addition, in the Griesbachian ocean, under warming climate conditions, lingulids in deeper water-depth environments might have been confronted with more intense competition for food and oxygen resources than in the shallower environment. This is reflected by reduced morphological disparity and shell size of lingulids in the Bozhou section, compared to increased morphological disparity and shell size of lingulids in the Liuzhi section. In the Dienerian to early Smithian, as environmental conditions improved, the morphological disparity and shell size of lingulids increased. The greatly increased shell size of lingulids from both sections in the Dienerian may have been a response to the rising predation intensity.

1. Introduction

Following a huge loss of biodiversity in the end-Permian Mass Extinction, recovery of marine ecosystems in the Early Triassic was sluggish (Jin et al., 2000; Shen et al., 2011; Fan et al., 2020). This has been attributed to persistently hostile environmental conditions, such as the largest perturbations of the carbon cycle in the Phanerozoic (Payne et al., 2004; Song et al., 2013; Du et al., 2022), deadly temperatures (Sun et al., 2012; Shen et al., 2018), and unbalanced spatial and temporal distribution of oceanic redox conditions (Pietsch and Bottjer, 2014; Huang et al., 2017; Zhang et al., 2018), in addition to the unique structure of oceanic ecosystems, represented by high dominance of the

benthic palaeocommunity (Boyer et al., 2004; Petsios and Bottjer, 2016; Pietsch et al., 2019).

In post-extinction benthic communities, ecological opportunist and disaster taxa rapidly filled vacant ecological niches (Chen and Benton, 2012) and restrained the evolutionary rate of benthos in the Early Triassic (Hautmann et al., 2015). These taxa include lingulid brachiopods, bivalve genera like *Unionites* and *Claraia* (Rodland and Bottjer, 2001; Petsios and Bottjer, 2016; Song et al., 2019; Huang et al., 2023), and microconchids (Shcherbakov et al., 2021). Lingulids were particularly remarkable in their proliferation during the Induan (early Early Triassic), and widely occur in numerous sections documenting onshore environments all over the world (Rodland and Bottjer, 2001; Peng and

* Corresponding author.

E-mail address: zhangy@cugb.edu.cn (Y. Zhang).

Shi, 2008). The unusually high number of lingulids also provides a crucial resource for investigating how these ecological opportunists adapted to the harsh marine environments during the post-extinction interval.

Lingulidae originated in the Late Devonian and still persist today (Carlson, 2016), and it is characterised by suboval outlines and simple concentric ornamentation (Emig and Herrera, 2006). Extant lingulids have an infaunal lifestyle associated with morphological characteristics such as the rearrangement of the mantle canals and reduction of pseudointerarea, and these traits are seen in extinct lingulids as far back as the Early Ordovician (Thayer and Steele-Petrović, 1975; Liang et al., 2023). Infaunal lingulid specimens have been found from a variety of strata in the Middle Ordovician, Upper Devonian and Triassic (Zonneveld et al., 2007; Harris and Gess, 2022; Liang et al., 2023).

Based on shell outline and shell size from successive strata in two sections of South China, this paper investigates morphospace (visualizations of morphological differences) and morphological disparity of shallower-water lingulids from the Griesbachian (early Induan) to Smithian (early Olenekian). The study aims to provide new insights into the morphological response of an important ecological opportunist to the environmental fluctuations of the Early Triassic.

2. Geological settings and age

The lingulid specimens analysed in this paper were sampled from two shallow-water sections in South China. The Bozhou section is located approximately 30 km southwest of Zunyi City, Guizhou Province, and the Liuzhi section is located about 15 km southwest of Liuzhi County, Guizhou Province. During the Early Triassic, the Bozhou and Liuzhi sections were situated at a transitional setting between the shallow-water clastic shelf and the shallow-water carbonate platform (Fig. 1). It is of note that the Bozhou section contains a higher percentage (around 50 %) of carbonate rocks than the Liuzhi section, which is consistent with its palaeogeographical location being much closer to the carbonate platform environment (Fig. 1).

The Bozhou section straddles the top of the Changxing Formation and the Yelang Formation (Fig. 2A). The Changxing Formation in this section is characterised by bioclastic limestone intercalated with claystone. The Yelang Formation is divided into three members, from its base to the top, the lowest Griesbachian Shabaowan Member, the lower–upper Griesbachian Yulongshan Member, and the uppermost

Griesbachian–lowermost Smithian Jiujitan Member (Chen et al., 2022). The Shabaowan member is characterised by yellowish-green calcareous mudstone intercalated with argillaceous limestone. The Yulongshan member is predominantly a limestone and argillaceous limestone unit, interbedded with some calcareous mudstone in the lower part. The Jiujitan member is dominated by purple massive silty and calcareous mudstone and argillaceous limestone interbeds. At the Bozhou section, the Permian–Triassic boundary (PTB) is located at the middle of Bed 7 in the uppermost part of the Changxing Formation based on the first occurrence of conodont *Hindeodus parvus*, and the Induan–Olenekian boundary is located at the base of Bed 49 in terms of the first occurrence of conodont *Eurygnathodus costatus* (Chen et al., 2022).

The Liuzhi section spans the interval from the uppermost Wangjiazhai Formation to the lower Yongningzhen Formation (Fig. 2B). The Wangjiazhai Formation is characterised by siliceous limestone in the lower part and silty and calcareous mudstone in the upper part. The Yelang Formation in this section is dominated by yellowish-green calcareous mudstone and limestone interbeds in the lower part, purple silty and calcareous mudstone interbedded with argillaceous limestone in the middle part, and purple silty and calcareous mudstone with sparsely dispersed limestone beds in the upper part. The Yongningzhen Formation from the section contains grey massive limestone and some purple silty and calcareous mudstone. Based on the correlations of PTB interval strata between the Bozhou and Liuzhi sections, the PTB of the Liuzhi section is placed between Bed 10 and Bed 11 (Chen et al., 2022). According to our unpublished data of bivalve biozones, the Induan–Olenekian boundary is located at the base of bed 50, which is also supported by lithological evidence that the Olenekian succession features massive light-grey limestone in south China (Tong et al., 2019).

3. Materials and methods

In this study, abundant lingulid specimens were systematically collected separately from the Bozhou and Liuzhi sections. These lingulids from the two studied sections belong to Family Lingulidae, and ‘lingulids’ mentioned in this paper all refers to Lingulidae. However, there are barely any internal traits (like muscle scars, visceral areas and pedicle nerves) preserved on most specimens (see Supplementary file A). Due to the very limited preservation of internal structures in the studied material, this study could not figure out detailed taxonomies and possible influences from the different muscle systems in the lingulid taxa

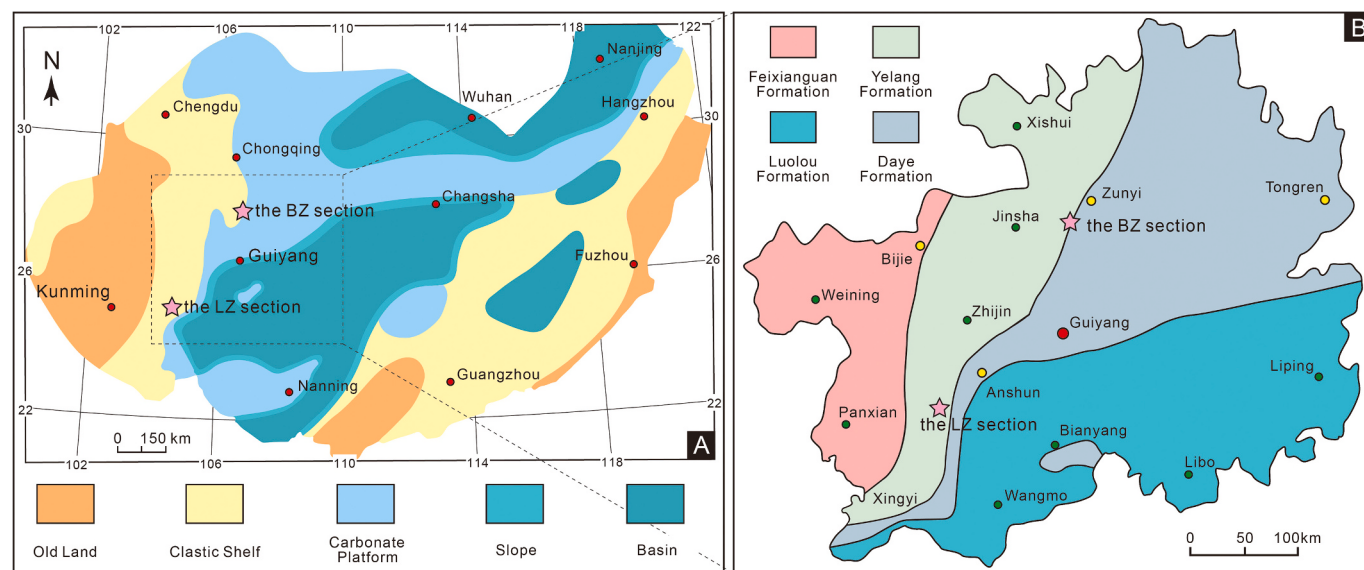


Fig. 1. (A) Palaeogeographical map of South China during the Early Triassic (modified from Feng et al., 1997), (B) Stratigraphy of Guizhou Province (modified from Bureau of Geology and Mineral Resources of Guizhou Province, 1987). The stars in the two images mark the locations of the Bozhou (BZ) and Liuzhi (LZ) sections.

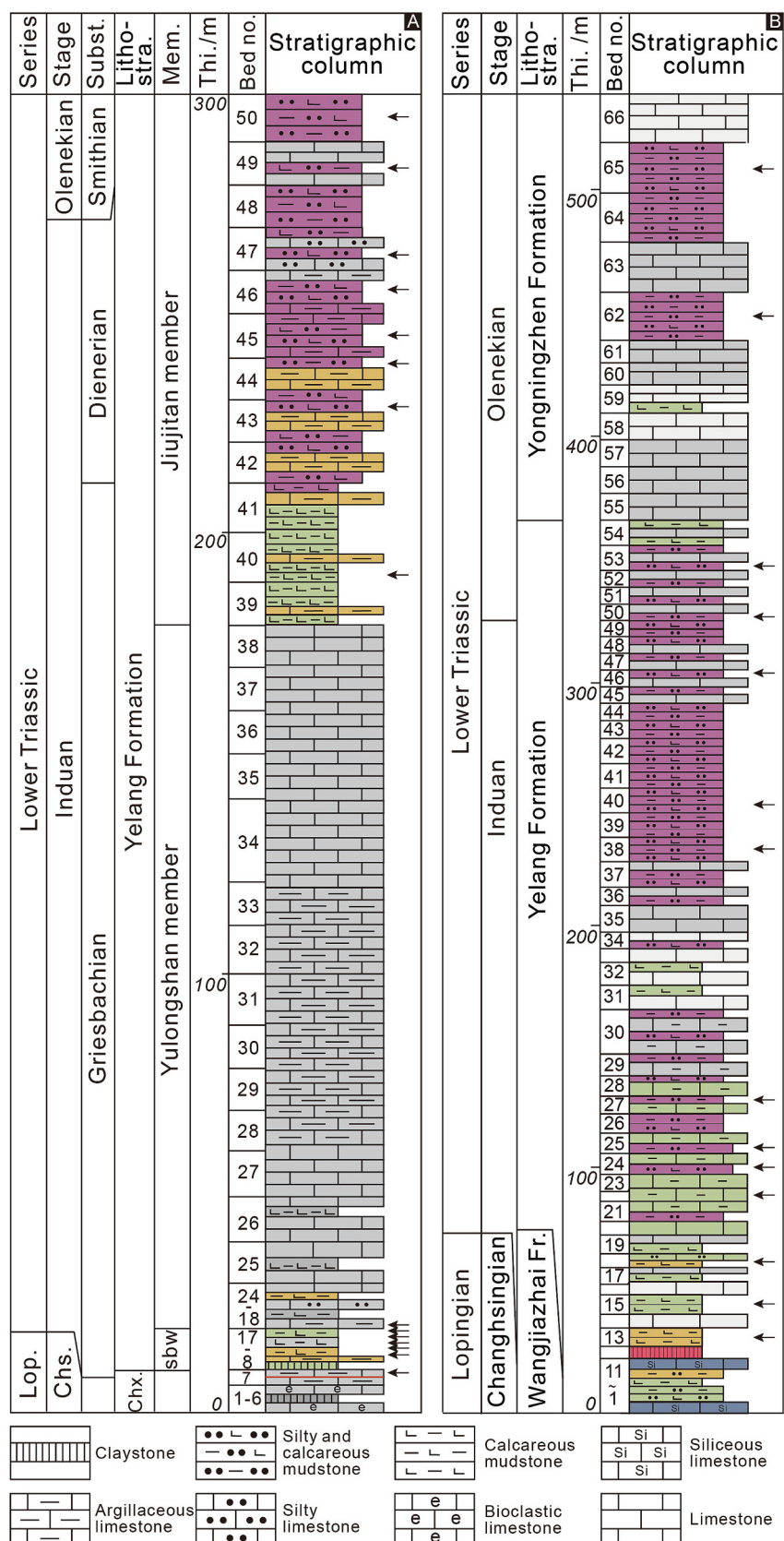


Fig. 2. Detailed stratigraphic log of the Bozhou section (A) and the Liuzhi section (B) showing lithology. Sampling intervals of lingulids are also marked.

included. All specimens analysed in this paper are stored in the School of Earth Sciences and Resources, China University of Geosciences (Beijing), China.

For each studied specimen, shell length and width were measured with a vernier caliper to the nearest 0.1 mm. Since lingulid brachiopods have an approximately elliptical shape, shell size was approximated with the product of π , half of shell length and half of shell width. In the shell size analysis, there are 476 specimens included from the Bozhou section, and 1054 specimens from the Liuzhi section. Box plots were produced for shell size data within stratigraphic intervals, aiming to show changes through time in both the Bozhou and Liuzhi sections, and the significance of size differences between adjacent bed intervals were checked with Mann-Whitney U tests. Both analyses were carried out using PAST (Hammer et al., 2001).

Almost all lingulid specimens from studied sections are preserved as mould fossils and internal structures are barely preserved. In addition, these lingulid specimens are basically consistent in the morphology along shell thickness. Therefore, the shape analyses here are based on geometric morphometric analyses of the two-dimensional outline profile of lingulid specimens. We conducted two separate analyses, one for samples from the Bozhou section, and another one just for Liuzhi samples. In both analyses, shape disparity was quantified using two-dimensional geometric landmarks, with a mixed landmark and semi-landmarks approach (Bookstein, 1991; Zelditch et al., 2012). One fixed landmark was positioned on all specimens as an anchoring point on the most posterior point, then 60 semi-landmark points were used to mark a curve representing the full external shape profile of each specimen (see Supplementary file A). Landmarks were digitized on images using tpsDig (Rohlf, 2006) by a single author (HW). Generalized Procrustes Analyses were applied to align all specimens and remove the noise effect of size, position, and rotation. Principal components analysis (PCA) was used on the aligned shape coordinates to visualise morphospace occupation for all specimens, using the R package *geomorph* (Adams et al., 2024). To observe the correspondence between locations in morphospace and shape change, morphometric shape transformation was projected into morphospace along major principal components, using the R package *morphospace* (Milla Carmona, 2024).

Morphospace occupation in different time intervals through both sections was explored in multiple ways. Firstly, nonparametric multivariate analysis of variance (NPMANOVA) was carried out on principal component scores (morphospace axes) partitioned into time intervals, to test whether the centroid and dispersion of specimens are different between selected intervals. Secondly, morphospace occupation in different intervals through the sections was illustrated by highlighting and plotting subsets of specimens found only in intervals of interest, and compared to the total sample for each section. Thirdly, we calculated the morphospace centroid location for selected intervals (representing the average position of all samples in that interval), and then plotted these centroid positions to illustrate how morphospace shifted through time in both sections. Finally, changes in morphological disparity in both sections were quantified by calculating the sum of variances disparity metric (Foote, 1992) for different intervals through the sections, using the R package *disparity* (Guillerme, 2018). The sum of variances is a widely used metric that quantifies disparity as the sum of the variance of each morphospace dimension (Wills, 2001). Compared to many disparity metrics derived from ordination axes, the sum of variances is relatively robust to differences in sample size (Giampaglio et al., 2001). Here, the sum of variances was calculated from all PC scores partitioned into different time intervals throughout the sections. 50 % and 95 % confidence intervals were generated for the disparity value in each interval based on 10,000 bootstrap replicates. Along with these confidence intervals, we also plot the mean disparity value derived from the bootstrap replicates. When analysing disparity changes through time, if interval bins have sample size less than three, the bins with low sample sizes were combined with their adjacent bins. There are respectively 162 and 358 specimens from the Bozhou and Liuzhi sections used for the

shape analysis. All these analyses were performed in R (R Development Core Team, 2016).

4. Results

4.1. Morphological variation of lingulids in the Bozhou section

Valve shape changes in the sampled lingulids are generally subtle modifications to their overall elliptical form. Nevertheless, morphospace of lingulid specimens from the Early Triassic of the Bozhou section shows some noteworthy changes in valve outline shape. PC1 and PC2 combined account for over 90 % of outline variation (Fig. 3). PC1 mainly reflects transformation from elongated outlines to compressed and rounded forms. PC1 also represents variation in the relative shape of the anterior and posterior margins, transitioning from having a similar curve shape in both margins, to having a posterior margin that is relatively more pointed than the anterior margin. PC2 reflects outline variation from common forms with rounded anterior margin and moderately pointed posterior margin, to those having rounder anterior margin and wider and less pointed posterior margin.

Based on morphospace occupation in different intervals and morphospace centroid movement through these intervals (Figs. 3 & 4), we discover that there are subtle morphological shifts when progressing up through the Bozhou section. Specimens from lower intervals are mainly distributed in the lower (negative PC2) regions, particularly the low right quadrant, and specimens from upper intervals are concentrated in the left upper region of morphospace. From the lower (beds 7–16) to upper (beds 40–50) intervals, lingulid valve outline shapes change from rounded triangular forms with moderately pointed posterior margins to forms with more narrow and elongated outlines and sometimes with posterior margins wider than the anterior margin (Fig. 3).

Within interval sum of variances disparity for lingulids from the Bozhou section through successive beds is presented, and disparity does not directly correspond to sample size (Fig. 5A). Overall, the morphological disparity of lingulids in the Bozhou section is high in the earliest Triassic, and decreased in the early Griesbachian. In the middle Griesbachian, disparity reaches the lowest point, and then increases continuously into the early Smithian (Fig. 5A). The overlapping confidence intervals associated with beds 40–43 to 49–50 suggest an insignificant disparity increase, but the disparity remains high during these intervals, which is consistent with the considerable expansion of overall morphospace occupation, especially for beds 40–43 and 44–47. From beds 7–9 to 13–14, morphospace occupation continuously shifts ($p = 0.002$ for beds 7–9 to 11, $p = 0.035$ for beds 11 to 13–14 in NPMANOVA test), followed by a nonsignificant change in bed 15–16 ($p = 0.191$ in NPMANOVA test). There is then another significant shift in morphospace between beds 15–16 to beds 40–43 ($p = 0.002$ in NPMANOVA test).

From bed 7–9 to bed 11, lingulid shell size significantly decreased, and the size range shrank considerably, followed by similarly low size range in bed 13–14 (Fig. 5B). From bed 15–16 to the topmost intervals of the Bozhou section, there is continuous and significant increase in lingulid shell size. In bed 49–50 the size range of and mean size of lingulids reached its highest point. It is worth noting that bed 18–38 in the Bozhou section is basically limestone and argillaceous limestone and thus there are no lingulid fossils found.

In brief, in the Bozhou section, the disparity and shell size of lingulids both declined significantly in the Griesbachian, and increased significantly in the Dienerian to early Smithian. In the early Smithian, disparity of lingulids finally stabilized in a range similar to that in the Griesbachian, but shell size continued to increase and had a wider range than that in the Griesbachian.

4.2. Morphological variation of lingulids in the Liuzhi section

In the Liuzhi section morphospace, PC1 and PC2 together account for

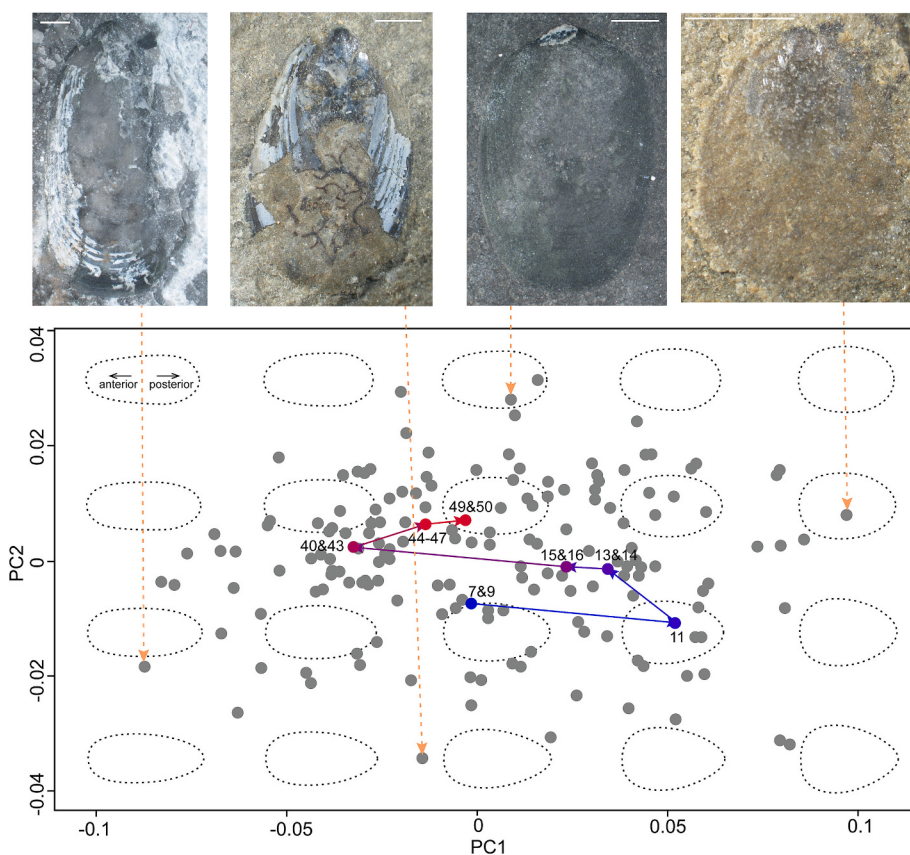


Fig. 3. Morphospace showing the distribution of all lingulid specimens in the Bozhou section. PC1 accounts for 86.4 % of total variation, and PC2 accounts for 9.4 % of total variation. The background shape illustrations show the landmark configurations in different parts of the morphospace. Specimens located at the margins of the morphospace are shown, and scale bars are 1 mm.

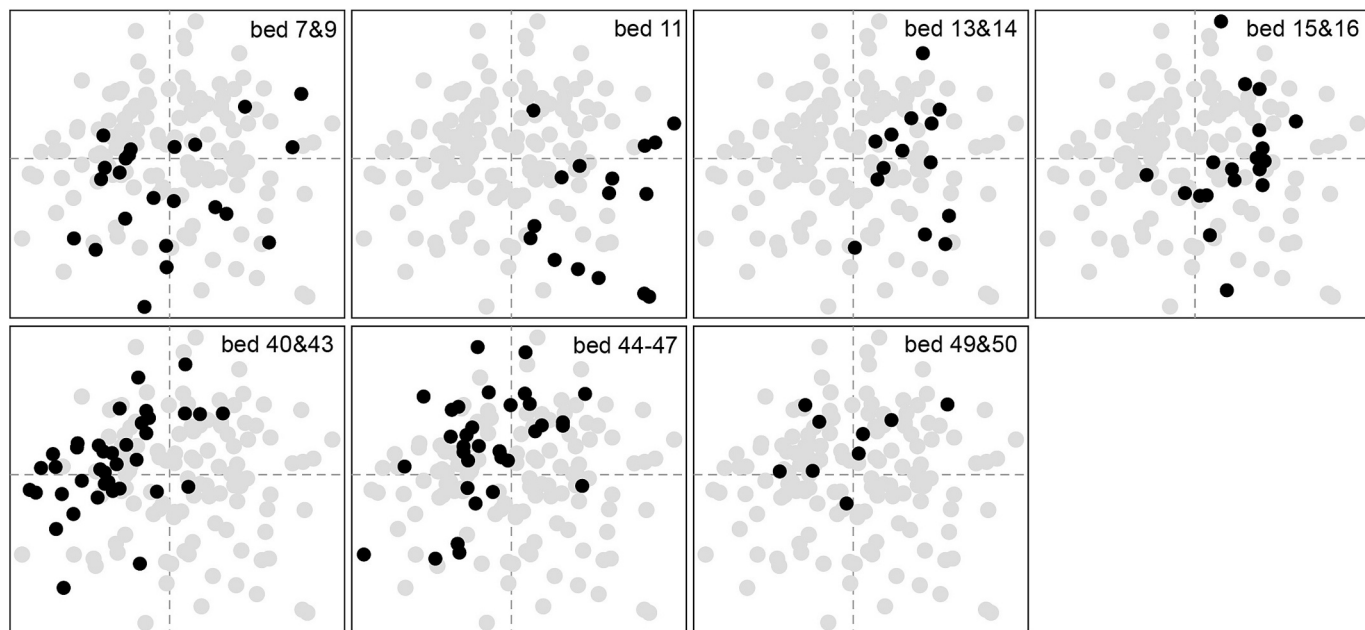


Fig. 4. Morphospace occupation of specimens from each interval of the Bozhou section based on principal components 1 and 2.

over 90 % of overall variance. PC1 represents variation in width/length ratio. Taxa with high positive PC1 scores have elongated suboval outline with pointed posterior ends (Fig. 6). Conversely, taxa with increasingly negative scores have short and rounded outlines, blunt posterior ends,

and wide and gentle anterior margins (Fig. 6). Variation in width and curvature of the posterior margin is strongly expressed on PC2. Taxa with high positive PC2 scores have moderate width/length ratio, but the anterior margin is wider than posterior margin. Taxa with increasingly

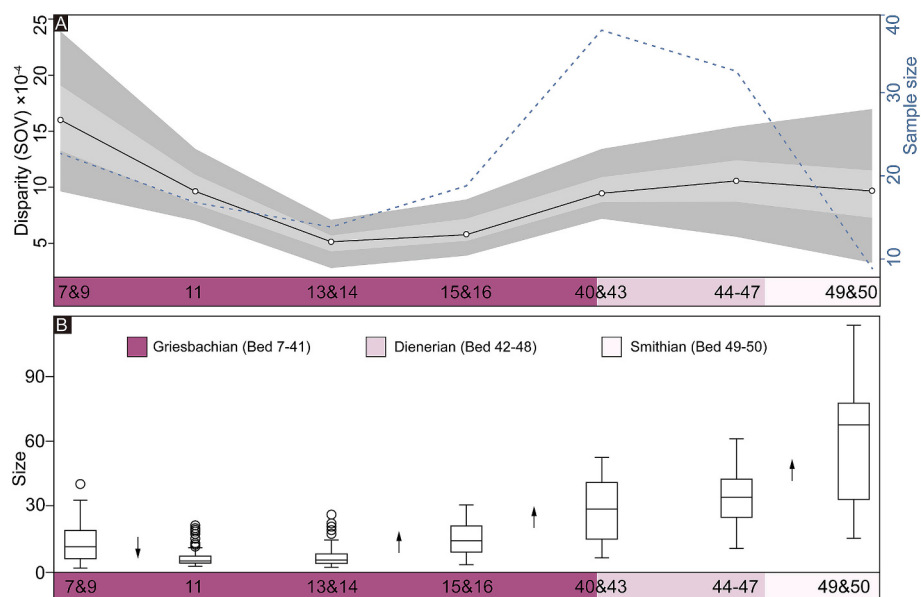


Fig. 5. (A) Disparity (sum of variances) of lingulids and the number of lingulid specimen (dashed line) from bed 7 to bed 50 in the Bozhou section. Mean disparity value are shown by the solid line with circles. The grey and dark grey envelopes represent 50 % and 95 % confidence intervals based on 10,000 bootstrap replicates. (B) Boxplot of lingulid shell size changes from bed 7 to bed 50 in the Bozhou section. Arrows show statistically significant changes based on Mann-Whitney U test.

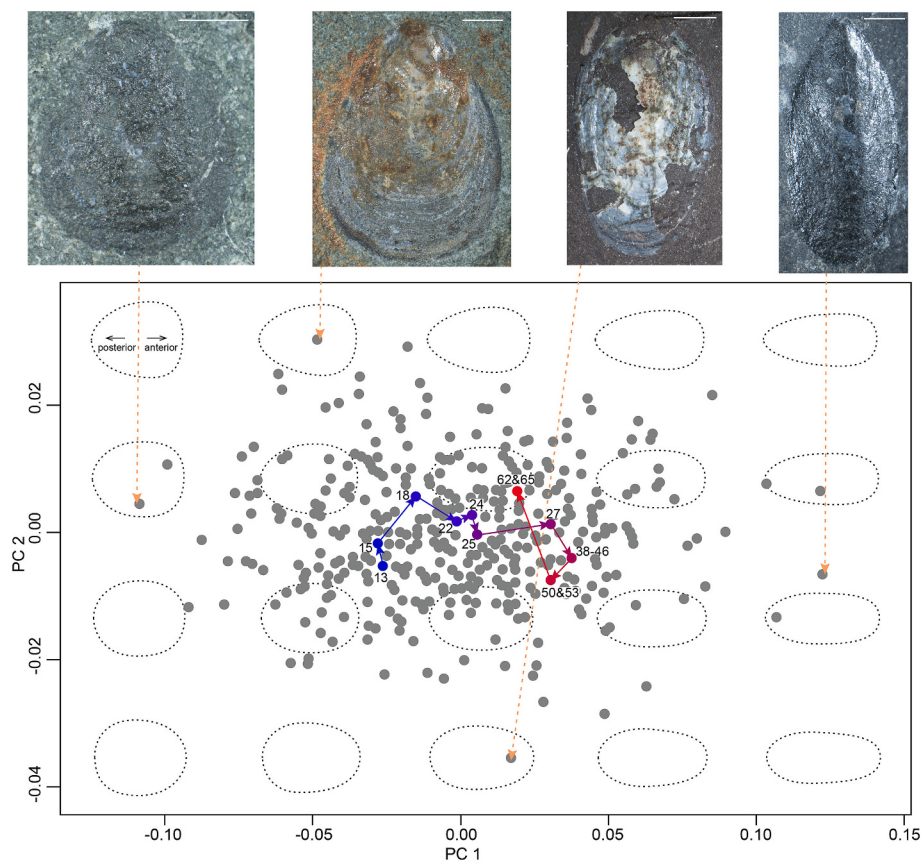


Fig. 6. Morphospace showing the distribution of all lingulid specimens in the Liuzhi section. PC1 accounts for 89.7 % of total variation, and PC2 accounts for 6.4 % of total variation. The background shape illustrations show the landmark configurations in different parts of the morphospace. Specimens located at the margins of the morphospace are shown, and scale bars are 1 mm.

negative PC2 scores have moderately pointed anterior margin with maximum shell width locating close to posterior margin (Fig. 6). Taxa from lower beds (beds 13–25) are mainly located in the left side of morphospace (negative PC1), mainly characterised by moderate

width/length ratios, and moderately rounded and gentle posterior ends (Fig. 6). Towards upper beds (beds 27–65), shapes are mostly concentrated in the right side of morphospace, showing notable expansion in the low right quadrant, and have low width/length ratio, and narrow

suboval to elongated subtriangular outlines, sometimes with posterior margins wider than anterior margins (Fig. 6). Although subtle, there is clearly a shift in morphospace along PC1 throughout the Liuzhi section.

Lingulids sum of variances disparity fluctuates from beds 13 to 25 in the Liuzhi section (Figs. 7 & 8). The marginal overlap of the confidence intervals in the sum of variances metric suggests that the increase and decline of disparity during these intervals are nonsignificant. Overall, morphospace occupation is relatively expansive and consistent from beds 13–25, especially for beds 13, 18, 24 and 25 (Fig. 8A). A significant morphospace shift is found between beds 25 and 27 ($p = 0.04$ in NPMANOVA test), when the total area of morphospace occupied also shrinks greatly and is concentrated in the right and lower parts (Figs. 7 & 8). The disparity decline and morphospace constriction found for bed 27 are also associated with a reduction in sample size. This may reflect poor sampling for this interval, or a genuine coupled decline in diversity and disparity. It is noteworthy that the constriction of morphospace that occurred in bed 27 is associated with the absence of all taxa from the left-side of morphospace (negative PC1) (Fig. 7), rather than the thinning-out of the previously occupied morphospace, or the random loss of taxa from all parts of morphospace. A shift in morphospace occupation then occurs between beds 27 and 38–46, and disparity also increases. In beds 50–65, disparity slightly declined, but the overlap of the confidence intervals in the sum of variances metric and statistical tests suggest that the disparity decline is nonsignificant (Fig. 8A).

Shell size of lingulids in the Liuzhi section significantly increases from beds 13 to 18, and then slightly rises in bed 22 (Fig. 8B). Despite a reduction in bed 24, the range of size then distinctly expands in bed 25, followed by a considerable rise of size in bed 27. From beds 27 to 46, the shell size significantly declines. From beds 50–65, the shell size shows significant increases and a great diversity of sizes. Overall, although fluctuations exist, lingulid shell size presents a consistent increasing trend, especially from bed 24 to the topmost intervals of the Liuzhi section.

To sum up, in the Liuzhi section, the disparity and shell size of lingulids both significantly increased in the Griesbachian, followed by a significant decrease in the middle Induan. In the Dienerian to early Smithian, the disparity rose to similar level of the Griesbachian, but mean shell size significantly increased and there was a much wider range of sizes.

5. Discussions

During the end-Permian mass extinction, lingulids experienced small diversity decline, but then showed a sharp increase in their occurrences in the Early Triassic (Carlson, 2016; our unpublished data of global

lingulids). According to Zonneveld et al. (2007), lingulids did not expand their habitats or environmental range in the post-extinction interval, which suggests they are ecological opportunists and mainly occupied the shallow and marginal marine clastic-shelf settings. Up to now, the reason why these special taxa could better adapt to the post-extinction marine environment remains unclear, although it could potentially involve both the biotic and environmental factors (McRoberts, 2001).

5.1. Adaptive changes in morphology from the early Induan to early Olenekian

Although lingulid brachiopods have been commonly considered as having an unchanged “linguliform” shape since they first appeared, their shape, which is tightly related with their burrowing lifestyle (Emig, 2003), is found to vary along with environmental changes in the Early Triassic. In both studied sections, lingulids from the early Griesbachian are mostly compressed and rounded with subtriangular outlines, and have narrow suboval outlines with small width/length ratios, with posterior margins sometimes wider than anterior margins in the late Induan and early Smithian. From the early Griesbachian to early Smithian, lingulid shell outlines become more elongated (Figs. 5 & 6 in Supplementary file A), and its anterior becomes narrower and even narrower than its posterior for some specimens (Fig. 9). The subtle changes in shell outline of lingulids highlights morphological adaptations, which could be attributed to both biotic and abiotic factors.

Although almost all lingulids of both sections are yielded from the clastic rocks of the Yelang Formation, the rocks from the lower part of both sections are mainly calcareous and silty mudstone, and those from the upper parts of both sections are characterised by silty mudstone, which contain distinctly coarser particles than the lower part. It has been previously shown that coarse sediment has a negative influence on both the burrowing capability and burrow depth of lingulids (Emig, 1982, 1997). Therefore, the environmental changes occurring from the Griesbachian to early Smithian at these two sections, mainly resulting in sediments becoming coarser, could have unfavorable effects on lingulids.

In addition, potential predators of lingulids, such as ophiuroid (Emig and Vargas, 1990), asteroid and crustaceans (Paine, 1963; Worcester, 1969; Culter, 1979; Emig and Vargas, 1990; Emig, 1997), and gastropods (Paine, 1963), are found to be more common in the late Early Triassic (McRoberts, 2001; Nützel, 2005; Twitchett and Oji, 2005; Braddy et al., 2017). Well-preserved ophiuroid fossils were found in Bed 40 of the Liuzhi section (unpublished materials), indicating the recovery of marine predators in this environmental setting.

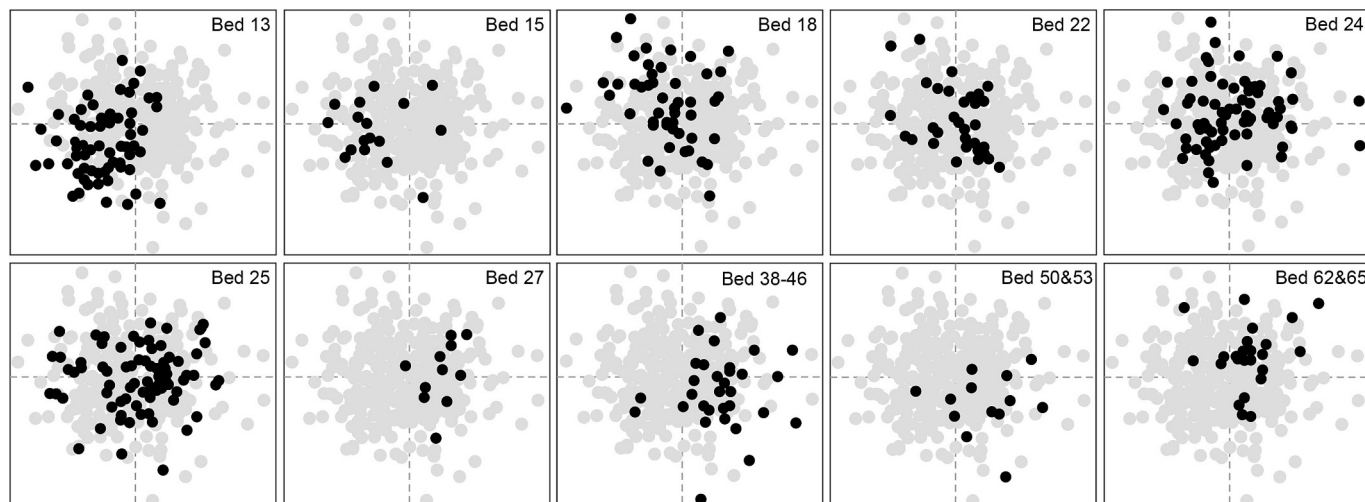


Fig. 7. Morphospace occupation of specimens from each interval of the Liuzhi section based on principal components 1 and 2.

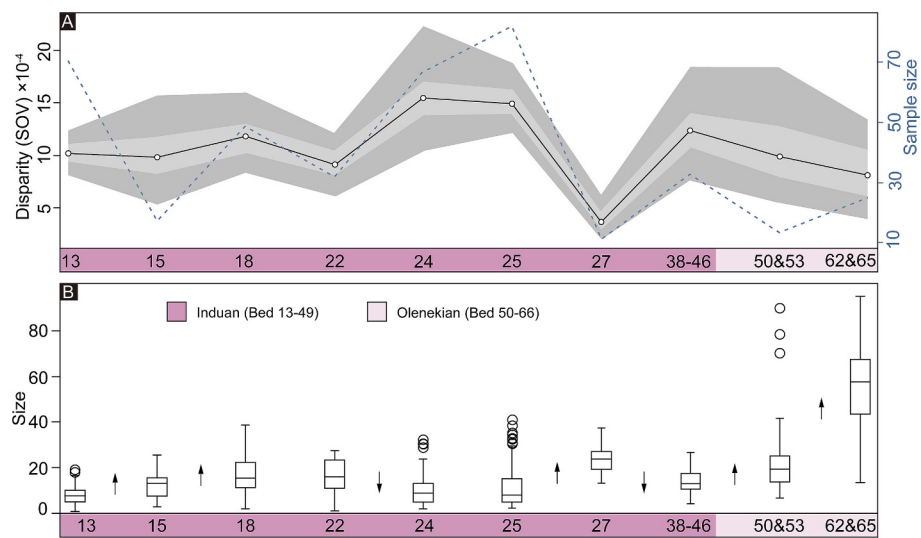


Fig. 8. (A) Disparity (sum of variances) of lingulids and the number of lingulid specimen (dashed line) from bed 13 to bed 65 in the Liuzhi section. Mean disparity value based are shown by the solid line with circles. The grey and dark grey envelopes represent 50 % and 95 % confidence intervals based on 10,000 bootstrap replicates. (B) Boxplot of lingulid shell size changes from bed 13 to bed 65 in the Liuzhi section. Arrows show statistically significant changes based on Mann-Whitney U test.

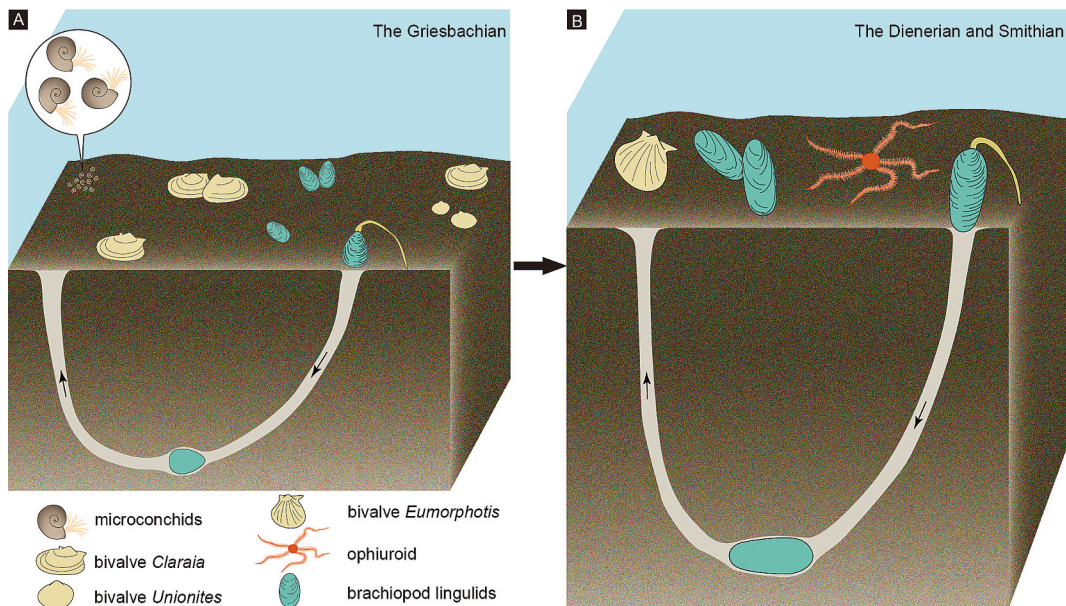


Fig. 9. Schematic reconstructions of the benthonic palaeocommunities during the Early Triassic. From A to B, shell size and shape of lingulids changed, and their burrows became deeper.

With increased intensity of predation accompanied by sediment particles becoming coarser, lingulid shape appears to have adaptably changed to improve their capacity to burrow and to retract into burrows. During the Dienerian to early Smithian, the lingulid shapes became slimmer with smaller width/length ratios (Fig. 9, Figs. 5 & 6 in Supplementary file A), which would make it easier to withdraw into and protrude out from their shelter (Peng et al., 2007). In addition, lingulids dig into the sediment by repeated scissorlike movements, shell closure with water injection, and shell openings by pressure pulses, while the posterior end of the shell is propped up by a stiffened pedicle and the anterior enters the sediment first (Thayer and Steele-Petrović, 1975; Emig, 1997, Fig. 9). From a mechanical and functional perspective, a narrower anterior part for lingulids equates to easier and faster digging into sediment, just like a shovel, which mostly also has a narrow and even pointed anterior end. Moreover, opening and closing movements of

the valves are generated by the contraction of muscles (Emig, 1997), which are distributed in the posterior part of shell. If the posterior area becomes wider, it might be able to provide more space to accommodate larger muscles, which can improve the opening and closing efficiency of the valves. Therefore, the major aspects of morphological variation documented for lingulids in this study, including the decreasing width/length ratio, relatively expanding posterior part and narrowing anterior part, might all be related to improving the capacity of burrowing and retracting to burrows.

5.2. Morphological disparity and shell size changes linked to different sedimentary environments

Extant *Lingula* use the protein hemerythrin that has an oxygen equilibrium which is reversibly altered by pH changes (Manwell, 1960),

and it can enable *Lingula* to store more oxygen when environments tend to be acidic. Like their modern relatives, lingulids may also have had such advantages to gain and store more oxygen than other organisms in the acidic and anoxic ocean during the Early Triassic (Knoll et al., 1996; Peng et al., 2007). As has already been observed in many other Early Triassic strata over the world (Powers and Bottjer, 2009), lingulids proliferated in the vacated habitats of shallow marine environment, reflected by the large sample sizes in the two studied sections (Figs. 5 & 8).

In the early Griesbachian, disparity and shell size changes for lingulids from the two studied sections showed different responses to environmental changes. Although both studied sections were situated in the shallow-water clastic rock shelf, the Liuzhi section was in a shallower water-depth environment than the Bozhou section, which was closer to the carbonate platform as is proved by the strata from the Bozhou section containing much more limestones. It has been previously shown that the early Induan ocean underwent a significant increase in temperature, and peaked at 38 °C in late Griesbachian (Sun et al., 2012). Initially, temperature increases might have greater impact on epifaunal organisms than infaunal organisms (Feder et al., 1994). Compared with those in the Liuzhi section, epifaunal groups in the Bozhou section should have been less affected, due to its relatively lower bottom temperature at deeper water-depth, which is supported by abundant microconchids in the early Griesbachian strata in the Bozhou section, but only very few of them occurred in the Liuzhi section (Jiang et al., 2024). Therefore, in the Bozhou section, disparity and mean shell size of lingulids significantly declined because of intense competition for food and oxygen resource, while disparity and shell size of lingulids significantly increased in the Liuzhi section in the early Griesbachian. Although the range of temperature tolerance of lingulids is highly variable, environments with a temperature about 38 °C are not favorable for modern lingulids (Emig, 1988, 1997). In late Griesbachian, when the seawater temperature reached a peak, both the disparity and shell size of lingulids in both studied sections significantly decreased.

In the Dienerian to early Smithian, the disparity and shell size of lingulids from both studied sections significantly increased, especially the shell size, which rose to a very high level. Similar increases of shell size and biodiversity in the Dienerian have been found in other studies (Twitchett, 2007; Hofmann et al., 2011; Posenato et al., 2014), and have been attributed to diminishing environmental stress. Additionally, the depth of burrow of lingulids is about ten times the length of the shell (Emig, 1997), so larger shells might indicate deeper burrows (Fig. 9). In modern ocean, case of the lingulid *Glottidia* being preyed upon by the asteroid *Luidia* are found mostly where shells are less than 1 cm long, which suggests that larger individuals might be hidden too deeply into sediment to be preyed upon (Emig, 1997). Therefore, the rising disparity and greatly increased shell size of lingulids from the Dienerian to early Smithian of both sections might be related with ameliorated environmental condition and the rising predation intensity mentioned above.

6. Conclusions

Morphology of shell outlines and shell size were investigated for lingulid specimens from two shallow-water sections of the Lower Triassic in South China. Our study documents the morphological response of an opportunistic taxon during the Early Triassic recovery interval. From the early Griesbachian to early Smithian, lingulids changed from short and rounded subtriangular outlines to elongated and narrow suboval outlines, and with posterior margins sometimes wider than anterior margins. These morphological changes relate to increased predation and sediments becoming coarse in the environment. In addition, in the Griesbachian ocean with increasing temperature, lingulids in the Bozhou section in deeper water-depth were confronted with fiercer competition than in the shallower Liuzhi section, and thus disparity and shell size of lingulids in the two sections showed opposite changes. In the Dienerian and early Smithian, with ameliorated environmental

conditions, shape disparity and shell size from both sections significantly increased.

CRediT authorship contribution statement

Huiting Wu: Writing – review & editing, Writing – original draft, Visualization, Validation, Methodology, Investigation, Funding acquisition, Formal analysis, Data curation, Conceptualization. **Thomas L. Stubbs:** Writing – review & editing, Writing – original draft, Visualization, Software, Methodology, Formal analysis. **Anfeng Chen:** Data curation. **Xiujuan Wu:** Data curation. **Yang Zhang:** Writing – review & editing, Writing – original draft, Validation, Investigation, Data curation, Conceptualization.

Declaration of competing interest

The authors declare that they have no known competing financial interests or personal relationships that could have appeared to influence the work reported in this paper.

Acknowledgements

We thank the journal editor, reviewer Sangmin Lee and another anonymous reviewer for their very valuable comments. This study has been supported by the National Natural Science Foundation of China (Grant No. 42372018), Fundamental Research Funds for the Central University (Grant No. 2023ZKPYDC03), and State Key Laboratory of Palaeobiology and Stratigraphy (Nanjing Institute of Geology and Palaeontology, CAS) (No. 223131).

Appendix A. Supplementary data

Supplementary data to this article can be found online at <https://doi.org/10.1016/j.palaeo.2025.113182>.

Data availability

The authors confirm that all data necessary for supporting the scientific findings of this paper have been provided.

References

- Adams, D.C., Collyer, M.L., Kaliontzopoulou, A., Baken, E.K., 2024. geomorph: Software for Geometric Morphometric Analyses. R Package Version 4.0.9. <https://cran.r-project.org/package=geomorph>.
- Bookstein, F.L., 1991. *Morphometric Tools for Landmark Data*. Cambridge University Press.
- Boyer, D.L., Bottjer, D.J., Droser, M.L., 2004. Ecological signature of lower Triassic shell beds of the western United States. *Palaios* 19, 372–380.
- Brayard, A., Krumenacker, L.J., Botting, J.P., Jenks, J.F., Bylund, K.G., Fara, E., Vennin, E., Olivier, N., Goudemand, N., Saucède, T., Charbonnier, S., Romano, C., Doguzhaeva, L., Thuy, B., Hautmann, M., Stephen, D.A., Thomazo, C., Escarguel, G., 2017. Unexpected early Triassic marine ecosystem and the rise of the modern evolutionary fauna. *Sci. Adv.* 3, e1602159.
- Bureau of Geology and Mineral Resources of Guizhou Province, 1987. *Regional Geology of Guizhou Province*. Geological Publishing House, Beijing, pp. 1–698 (in Chinese with English abstract).
- Carlson, S.J., 2016. The evolution of Brachiopoda. *Annu. Rev. Earth Planet. Sci.* 44, 409–438.
- Chen, Z.Q., Benton, M.J., 2012. The timing and pattern of biotic recovery following the end-Permian mass extinction. *Nat. Geosci.* 5, 375–383.
- Chen, A.F., Zhang, Y., Yuan, D.X., Wu, H.T., Dou, J., Liu, J.Q., 2022. Upper Changhsingian to lower Olenekian conodont successions from the Bozhou section, northern Guizhou Province, southwestern China. *Palaeogeogr. Palaeoclimatol. Palaeoecol.* 599, 111054.
- Ciampaglio, C.N., Kemp, M., McShea, D.W., 2001. Detecting changes in morphospace occupation patterns in the fossil record: Characterization and analysis of measures of disparity. *Paleobiology* 27, 695–715.
- Culter, J.M., 1979. A Population Study of the Inarticulate Brachiopod *Glottidia pyramidata* (Stimpson). University of South Florida, Tampa, p. 53. Master's thesis (non publié).
- Du, Y., Zhu, Y.Y., Corso, J.D., Huang, J.D., Qiu, H.O., Song, H.J., Tian, L., Chu, D.L., Tong, J.N., Song, H.Y., 2022. New early Triassic marine δ¹³C record from the

- northeastern Yangtze Platform: implications for contemporaneous temperature changes and volcanic eruptions. *Palaeogeogr. Palaeoclimatol. Palaeoecol.* 607, 111270.
- Emig, C.C., 1982. Terrier et position des lingules (brachiopodes, inarticulés). *Bull. Soc. Zool. Fr.* 107, 185–194.
- Emig, C.C., 1988. Les brachiopodes actuels sontils des indicateurs (paléo) bathymétriques? *Géol. Médit.* 15, 65–71.
- Emig, C.C., 1997. Ecology of the inarticulated brachiopods. In: Williams, A., Brunton, C.H., Carlson, S.J., et al. (Eds.), *Treatise on Invertebrate Paleontology*. Part H. Brachiopoda, vol. 1. Geological Society of America and University of Kansas, Boulder, Colorado, and Lawrence, Kansas, pp. 473–495 (Revised).
- Emig, C.C., 2003. Proof that Lingula (Brachiopoda) is not a livingfossil, and emended diagnoses of the family Lingulidae. In: Notebooks on Geology-Letter 2003/01.
- Emig, C.C., Herrera, Z., 2006. Dignomia munsterii (Brachiopoda, Lingulata) from the Ordovician of Bolivia, with redescription of the genus. *Geodiversitas* 28, 227–237.
- Emig, C.C., Vargas, J.A., 1990. Notes on Glottidia audebarti (Broderip) (Brachiopoda, Lingulidae) from the Gulf of Nicoya, Costa Rica. *Rev. Biol. Trop.* 38, 251–258.
- Fan, J.X., Shen, S.Z., Erwin, D.H., Sadler, P.M., MacLeod, N., 2020. A high-resolution summary of Cambrian to early Triassic marine invertebrate biodiversity. *Science* 367, 272–277.
- Feder, H.M., Foster, N.R., Jewett, S.C., Weingartner, T.J., Baxter, R., 1994. Mollusks in the northeastern Chukchi Sea. *Arctic* 1455–1463.
- Feng, Z.Z., Yang, Y.Q., Jin, Z.K., Li, S.W., Bao, Z.D., 1997. Lithofacies Paleogeography of Permian of South China. Petroleum University Press, Dongying (Shandong Province), pp. 1–242 (in Chinese with English abstract).
- Foote, M., 1992. Rarefaction analysis of morphological and taxonomic diversity. *Paleobiology* 18, 1–16.
- Guillerme, T., 2018. dispRity: a modular R package for measuring disparity. *Methods Ecol. Evol.* 9, 1755–1763.
- Hammer, Ø., Harper, D.A.T., Ryan, P.D., 2001. PAST: Paleontological statistics software package for education and data analysis. *Palaeontol. Electron.* 4, 1–9.
- Harris, C., Gess, R.W., 2022. Insights from a monospecific lingulid brachiopod bed in the late Devonian of South Africa. *Palaios* 37, 471–485.
- Hautmann, M., Bagherpour, B., Brosse, M., Frisk, A., Hofmann, R., Baud, A., Nützel, A., Goudemand, N., Bucher, H., 2015. Competition in slow motion: the unusual case of benthic marine communities in the wake of the end-Permian mass extinction. *Palaeontology* 58, 871–901.
- Hofmann, R., Goudemand, N., Wasmer, M., Bucher, H., Hautmann, M., 2011. New trace fossil evidence for and early recovery signal in the aftermath of the end-Permian mass extinction. *Palaeogeogr. Palaeoclimatol. Palaeoecol.* 310, 216–226.
- Huang, Y.G., Chen, Z.Q., Wignall, P.B., Zhao, L.S., 2017. Latest Permian to Middle Triassic redox condition variations in ramp settings, South China: pyrite frambooid evidence. *GSA Bull.* 129, 229–243.
- Huang, Y.F., Tong, J.N., Tian, L., Song, H.J., Chu, D.L., Miao, X., Song, T., 2023. Temporal shell-size variations of bivalves in South China from the late Permian to the early Middle Triassic. *Palaeogeogr. Palaeoclimatol. Palaeoecol.* 609, 111307.
- Jiang, G.F., Liu, J.Q., Chen, A.F., Lyu, W.B., Zhang, H., Zhang, Y., 2024. Early Triassic microconchids in shallow-water clastic facies from western Guizhou Province and its palaeoecological significance. *Acta Palaeontol. Sin.* 63, 94–101.
- Jin, Y.G., Wang, Y., Wang, W., Shang, Q.H., Cao, C.Q., Erwin, D.H., 2000. Patterns of mass extinction near the Permian-Triassic boundary in South China. *Science* 289, 432–436.
- Knoll, A.H., Bambach, R.K., Canfield, D.E., Grotzinger, J.P., 1996. Comparative earth history and late Permian mass extinction. *Science* 273, 452–457.
- Liang, Y., Strotz, L.C., Topper, T.P., Holmer, L.E., Budd, G.E., Chen, Y.L., Fang, R.S., Hu, Y.Z., Zhang, Z.F., 2023. Evolutionary contingency in lingulid brachiopods across mass extinctions. *Curr. Biol.* 33, 1565–1572.
- Manwell, C., 1960. Oxygen equilibrium of brachiopod *Lingula hemerythrin*. *Science* 132, 550–551.
- McRoberts, C.A., 2001. Triassic bivalves and the initial marine Mesozoic revolution: a role for predators? *Geology* 29, 359–362.
- Milla Carmona, P., 2024. Morphospace: Build, Visualize and Explore Multivariate Ordinations of Shape Data. <https://github.com/millacarmona/morphospace>. <http://millacarmona.github.io/morphospace/>.
- Nützel, A., 2005. A new early Triassic gastropod genus and the recovery of gastropods from the Permian/Triassic extinction. *Acta Palaeontol. Pol.* 50, 19–24.
- Paine, R.T., 1963. Ecology of the brachiopod *Glottidia pyramidata*. *Ecological monographs* 33, 187–213.
- Payne, J.L., Lehrmann, D.J., Wei, J.Y., Orchard, M.J., Schrag, D.P., Knoll, A.H., 2004. Large perturbations of the carbon cycle during recovery from the end-Permian extinction. *Science* 305, 506–509.
- Peng, Y.Q., Shi, G.R., 2008. New early Triassic Lingulidae (Brachiopoda) genera and species from South China. *Alcheringa* 32, 149–170.
- Peng, Y.Q., Shi, G.R., Gao, Y.Q., He, W.H., Shen, S.Z., 2007. How and why did the Lingulidae (Brachiopoda) not only survive the end-Permian mass extinction but also thrive in its aftermath? *Palaeogeogr. Palaeoclimatol. Palaeoecol.* 252, 118–131.
- Petsios, E., Bottjer, D.J., 2016. Quantitative analysis of the ecological dominance of benthic disaster taxa in the aftermath of the end-Permian mass extinction. *Paleobiology* 42, 380–393.
- Pietsch, C., Bottjer, D.J., 2014. The importance of oxygen for the disparate recovery patterns of the benthic macrofauna in the early Triassic. *Earth Sci. Rev.* 137, 65–84.
- Pietsch, C., Ritterbush, K.A., Thompson, J.R., Petsios, E., 2019. Evolutionary models in the early Triassic marine realm. *Palaeogeogr. Palaeoclimatol. Palaeoecol.* 513, 65–85.
- Posenato, R., Holmer, L.E., Prinot, H., 2014. Adaptive strategies and environmental significance of lingulid brachiopods across the late Permian extinction. *Palaeogeogr. Palaeoclimatol. Palaeoecol.* 399, 373–384.
- Powers, C.M., Bottjer, D.J., 2009. Behavior of lophophorates during the end-Permian mass extinction and recovery. *J. Asian Earth Sci.* 36, 413–419.
- R Development Core Team, 2016. R: A language and environment for statistical computing. R Foundation for Statistical Computing, Vienna, Austria.
- Rodland, D.L., Bottjer, D.J., 2001. Biotic recovery from the end-Permian mass extinction: behavior of the inarticulate brachiopod Lingula as a disaster Taxon. *Palaios* 16, 95–101.
- Rohlf, F.J., 2006. tpsDig, Version 2.10. Department of Ecology and Evolution, State University of New York, Stony Brook, New York.
- Shcherbakov, D.E., Vinn, O., Zhuravlev, A.Y., 2021. Disaster microconchids from the uppermost Permian and lower Triassic lacustrine strata of the Cis-Urals and the Tunguska and Kuznetsk basins (Russia). *Geol. Mag.* 158, 1335–1357.
- Shen, S.Z., Crowley, J.L., Wang, Y., Bowring, S.A., Erwin, D.H., Sadler, P.M., Cao, C.Q., Rothman, D.H., Henderson, C.M., Ramezani, J., Zhang, H., Shen, Y.N., Wang, X.D., Wang, W., Mu, L., Li, W.Z., Tang, Y.G., Liu, X.L., Liu, L.J., Zeng, Y., Jiang, Y.F., Jin, Y.G., 2011. Calibrating the end-Permian mass extinction. *Science* 334, 1367–1372.
- Shen, S.Z., Ramezani, J., Chen, J., Cao, C.Q., Erwin, D.H., Zhang, H., Xiang, L., Schoepfer, S.D., Henderson, C.M., Zheng, Q.F., Bowring, S.A., Wang, Y., Li, X.H., Wang, X.D., Yuan, D.X., Zhang, Y.C., Mu, L., Wang, J., Wu, Y.S., 2018. A sudden end-Permian mass extinction in South China. *GSA Bull.* 131, 205–223.
- Song, H.Y., Tong, J.N., Algeo, T.J., Horacek, M., Qiu, H.O., Song, H.J., Tian, L., Chen, Z.Q., 2013. Large vertical 813CDIC gradients in early Triassic seas of the South China craton: Implications for oceanographic changes related to Siberian Traps volcanism. *Global Planet. Change* 105, 7–20.
- Song, T., Tong, J.N., Tian, L., Chu, D.L., Huang, Y.F., 2019. Taxonomic and ecological variations of Permian-Triassic transitional bivalve communities from the littoral clastic facies in southwestern China. *Palaeogeogr. Palaeoclimatol. Palaeoecol.* 519, 108–123.
- Sun, Y.D., Joachimski, M.M., Wignall, P.B., Yan, C.B., Chen, Y.L., Jiang, H.S., Wang, L.N., Lai, X.L., 2012. Lethally hot temperatures during the early Triassic greenhouse. *Science* 338, 366–370.
- Thayer, C.W., Steele-Petrović, H.M., 1975. Burrowing of the lingulid brachiopod *Glottidia pyramidata*: its ecologic and paleoecologic significance. *Lethaia* 8, 209–221.
- Tong, J.N., Chu, D.L., Liang, L., Shu, W.C., Song, H.J., Song, T., Song, H.Y., Wu, Y.Y., 2019. Triassic integrative stratigraphy and timescale of China. *Sci. China Earth Sci.* 62, 189–222.
- Twitchett, R.J., 2007. The Lilliput effect in the aftermath of the end-Permian extinction event. *Palaeogeogr. Palaeoclimatol. Palaeoecol.* 252, 132–144.
- Twitchett, R.J., Oji, T., 2005. Early Triassic recovery of echinoderms. *Comp. Rend. Palevol.* 4, 531–542.
- Wills, M.A., 2001. Morphological disparity: A primer. In: *Fossils, Phylogeny, and Form*. Springer US, Boston, MA, pp. 55–144.
- Worcester, W., 1969. On Lingula reevi. Unpublished M.S. thesis. Univ. Hawaii, p. 49.
- Zelditch, M.L., Swiderski, D.L., Sheets, H.D., 2012. *Geometric Morphometrics for Biologists: A Primer*, 2nd ed. Academic Press.
- Zhang, F.F., Romaniello, S.J., Algeo, T.J., Lau, K.V., Clapham, M.E., Richoz, S., Herrmann, A.D., Smith, H., Horacek, M., Anbar, A.D., 2018. Multiple episodes of extensive marine anoxia linked to global warming and continental weathering following the latest Permian mass extinction. *Sci. Adv.* 4, e1602921.
- Zonneveld, J.P., Beatty, T.W., Pemberton, S.G., 2007. Lingulid brachiopods and the trace fossil lingulichnus from the Triassic of Western Canada: implications for faunal recovery after the end-Permian mass extinction. *Palaios* 22, 74–97.